Dalton Transactions

PAPER

View Article Online
View Journal | View Issue

Cite this: *Dalton Trans.*, 2017, **46**, 8727

A structural study of alkaline earth metal complexes with hybrid disila-crown ethers†

Fabian Dankert, Kirsten Reuter, Carsten Donsbach and Carsten von Hänisch*

Received 19th October 2016,
Accepted 24th November 2016

DOI: 10.1039/c6dt04018g

rsc.li/dalton

Compounds consisting of $[M(1,2\text{-disila-}[3n]\text{crown-}n)]^{2+}$ (M = Mg, Ca, Sr, Ba; n = 5, 6) and $[Ba(1,2\text{-disila-benzo}[18]\text{crown-}6)]^{2+}$ cations and different anions were obtained by equimolar reaction of the hybrid disila-crown ethers 1,2-disila[15]crown-5 (**1**), 1,2-disila[18]crown-6 (**2**) and 1,2-disila-benzo[18]crown-6 (**7**) with alkaline earth metal salts. Even with strongly coordinating anions such as Br^- or I^- stable complexes could be obtained, showing the good coordination ability of these ligands. The structures of all coordination compounds were determined *via* single crystal X-ray diffraction (XRD). By means of DFT calculations, the complexation ability of 1,2-disila[15]crown-5 (**1**) towards magnesium bromide was determined to be considerably higher compared to [15]crown-5. The opposite case was observed in solution as the exchange of calcium cations between [18]crown-6 and 1,2-disila[18]crown-6 (**2**) was studied *via* dynamic proton nuclear magnetic resonance (NMR) spectroscopy.

Introduction

Within the scope of developing macrocycles, there has also been an increased interest in ring compounds which are made of an inorganic skeleton.[1–3] Unlike crown ether complexes, coordination compounds with cyclosiloxanes are very rare. They are mostly constituted of a weakly coordinating anion such as Al_F (Al_F = $[Al\{OC(CF_3)_3\}_4]^-$), $[SbF_6]^-$ or $[InH\{CH_2C(CH_3)\}_3]^-$ as counterion where the charge is widely spread over a non-nucleophilic, chemically robust moiety.[2,4–6] The Zr(IV) compound $[Zr(D_6)Br_2][Zr_2Br_9]_2$ (D = Me_2SiO) is a unique example of a cyclosiloxane complex with a more strongly coordinating halide anion.[7]

One model to describe the reduced basicity of siloxanes is the negative hyperconjugation. An occupied p-orbital of the oxygen atom donates electron density into the σ*-orbital of the silicon–methyl bond, which strengthens the Si–O bond. The complexation of metal ions leads to a competing polarization.[2,8] According to Weinhold and West, negative hyperconjugation plays a major role in permethylated siloxanes, which was recently shown *via* natural-bond-orbital-analysis.[9,10] Another approach to explain the low basicity of siloxanes consists of an ionic consideration of the Si–O bond.[11–13] Despite the high anionicity of the O atoms, siloxanes do not exhibit an increased coordination ability owing to the energetically unfavoured further polarisation of the already polar Si–O bond. In this respect changes in the $n_O \rightarrow \sigma^*_{Si-C}$ interaction play a significant role.[8] Recent work suggests that repulsion between the positively polarized Si atom and the metal ion is eminently important beside the negative hyperconjugation to explain the low coordination ability of cyclosiloxanes.[14] Furthermore, extraction experiments have shown that the complexation abilities of ring contracted crown ethers like [17]crown-6 and sila[17]crown-6 are notably smaller than those of common crown ethers revealing that not only electronic effects but also the conformation of the macrocycle determines the complexation ability of such compounds.[15,16]

These facts motivated us to incorporate a Si_2Me_4 unit rather than one $SiMe_2$ in between the oxygen atoms of crown ethers (Scheme 1). Less attention has been paid to this function and its coordination chemistry even though it is known for quite some time.[17,18] However, in our recent work on hybrid disila-crown ethers we were able to synthesize crown ethers of the type 1,2-disila[3*n*]crown-*n* and their alkali metal complexes. The reaction of 1,2-dichloro-1,1,2,2-tetramethyldisilane and the appropriate glycole yielded the hybrid crown ether.

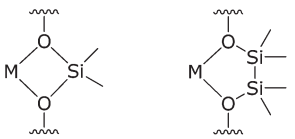

Scheme 1 Binding modes of siloxanes (left) and disila-crowns (right) in metal complexes.

Fachbereich Chemie and Wissenschaftliches Zentrum für Materialwissenschaften (WZMW), Philipps-Universität Marburg, Hans-Meerwein-Straße 4, D-35032, Marburg, Germany. E-mail: haenisch@chemie.uni-marburg.de

†Electronic supplementary information (ESI) available. CCDC 1497467–1497471. For ESI and crystallographic data in CIF or other electronic format see DOI: 10.1039/c6dt04018g

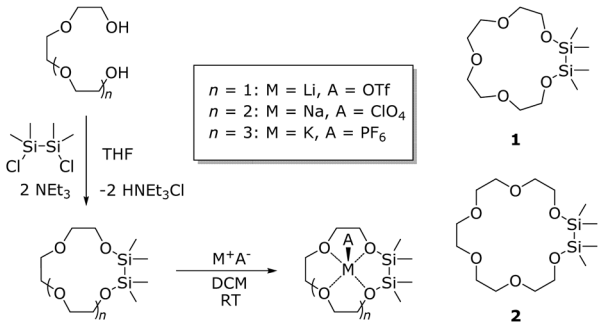

Scheme 2 Synthesis of hybrid disila-crown-ethers and their alkali metal complexes.

Complexation with selected alkali metal salts in dichloromethane (DCM) then yielded their alkali metal complexes (Scheme 2). By means of DFT calculations as well as dynamic proton NMR experiments, we revealed a comparable complexation ability of these crown ethers and their organic analogues.[19] We therefore assume that the reduced complexation ability of siloxanes is rather the result of structural and electrostatic factors. As the next step in understanding the coordination chemistry of disila-crown ethers we herein report the incorporation of alkaline earth metal cations.

Results and discussion

Treatment of **1** with $MgBr_2$ in trifluorotoluene led to the coordination compound [Mg(1,2-disila[15]crown-5)Br_2] (**3**). Neat **3** is a white powder which can be recrystallized after dissolution in DCM and layering with *n*-pentane. The resulting colourless plates were analysed *via* XRD. **3** crystallizes in the orthorhombic space group *Pbca*. The magnesium cation is coordinated by all oxygen atoms of the cyclic ligand as well as by two bromide ions giving a coordination number of seven (Fig. 1). The oxygen atoms are in almost coplanar arrangement with the magnesium cation, which is apparent from the Br1–Mg1–O-angles of approximately 90°. The $MgBr_2$ fragment is in well-nigh linear shape showing a Br1–Mg1–Br2 angle of 178.5(1)°. This is consistent with the [$Mg(THF)_4Br_2$] (THF = tetrahydrofuran) complex, whose Br–Mg–Br-angle is 178.0(1)°.[20]

The O–Mg–O-angles differ from 67.5(1) to 81.5(1)°. The O1–Mg1–O5-angle is enlarged as a result of the Si–Si bond of 232.2(1) pm. The methyl groups are taking an almost ecliptic arrangement, which can be seen in the C–Si–Si–C-torsion angles of 9.3(1)° and 6.2(1)°. This eclipsed arrangement was also reported for different cyclosiloxane and disila-crown ether complexes.[2,4,14,19,21] The O–Mg-bond lengths vary from 223.3(2) to 235.1(2) pm. Hence they are slightly longer than the O–Mg-bond lengths in related compounds with [15]crown-5 as ligand (see Table 1) and quite as long as those of [Mg([18]crown-6)(Cl–H–Cl)$_2$].[22] However, the O–Mg-bond lengths of fully carbon substituted oxygen atoms in **3** are comparable to those which are half carbon and half silicon substituted, so there is no hint for lower complexation ability of the silicon bonded oxygen atoms.

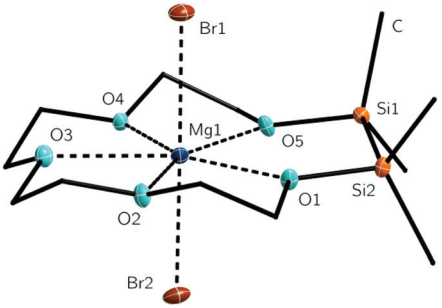

Fig. 1 Molecular structure of **3** in the crystal. Thermal ellipsoids represent a probability level of 50%. Hydrogen atoms are omitted for clarity. Selected bond lengths [pm]: O1–Mg1 227.5(2), O2–Mg1 225.3(2), O3–Mg1 235.1(2), O4–Mg1 223.8(2), O5–Mg1 222.3(2), Br1–Mg1 260.9(1), Br(2)–Mg1 258.9(1), Si1–O5 168.9(2), Si2–O1 168.5(2), Si1–Si2 232.3(1). Selected bond angles [°]: O1–Mg1–O5 81.5, O1–Mg1–Br1 88.8(1), O2–Mg1–Br1 89.2(1), O3–Mg1–Br1 88.9(1), O4–Mg1–Br1 91.4(1), O5–Mg1–Br1 89.5(1), Br1–Mg1–Br2 178.5(1).

Table 1 Selected bond lengths [pm] for compounds **3–5** and their related crown ether complexes

Compound	O_{crown}–M [pm]	CN[a]	Ref.
3	223.3(2)–235.1(2)	7	*b*
[Mg([15]crown-5)($SCPh_3$)$_2$]	214.3(3)–219.2(4)	7	26
[Mg([15]crown-5)(H_2O)$_2$](NO_3)$_2$	201.2(7)–235.7(8)	7	27
[Mg([15]crown-5)(NCS)$_2$]	214.2(2)–223.9(7)	7	28
[Mg([15]crown-5)([$CuCl_4$])CH_3CN]	211.7(4)–219.1(3)	7	29
4	243.6(1)–247.9(1)	7	*b*
[Ca([18]crown-6)(OTf)$_2$(H_2O)]	255.5(1)–265.7(1)	9	30
[Ca([18]crown-6)I_2]	264.9(5)[c]	8	31
[Ca([15]crown-5)(NCS)$_2$$H_2O$]	251.2(2)–258.5(2)	8	28
[Ca([15]crown-5)(NO_3)$_2$]	247.4(3)–258.1(4)	9	27
5	270.0(2)–277.7(2)	8	*b*
[Sr([18]crown-6)(NO_3)$_2$]	266.7(5)–275.5(3)	10	27
[Sr([18]crown-6)(HSO_4)$_2$]	268.2(8)–268.0(8)	10	32
[Sr([18]crown-6)(H_2O)$_3$][$CuCl_4$]	267.2(3)–270.0(3)	9	33
[Sr([18]crown-6)($MeCN$)$_3$][BPh_4]$_2$	262.4(2)–271.4(2)	9	34
[Sr([18]crown-6)(hmpa)$_2$][$Sn(SnPh_3)_3$]$_2$	258.9(4)–273.6(4)	8	35

[a] Coordination number. [b] This work. [c] All symmetry generated.

The shortest O–Mg bond is attributed to the silicon bonded oxygen atom O5 whereas the longest O–Mg bond is observed for the fully carbon substituted oxygen atom O3. The relative binding affinity of the hybrid ligand **1** towards magnesium bromide was further studied by quantum chemical calculations and is presented in Scheme 3. The exchange of magnesium bromide from [15]crown-5 to 1,2-disila[15]crown-5 (**1**) was calculated by means of DFT using the BP86 functional and def2-TZVP basis sets with inclusion of dispersion interactions together with charge compensation and is energetically favoured by 217.63 kJ mol^{-1}. This result implies a significantly better coordination ability of **1** compared to [15]crown-5 and is in well accordance to previous calculations for 1,2-disila[12]crown-4 towards Li^+.[19] Unfortunately, the results of quantum chemical calculations could not be underlined with

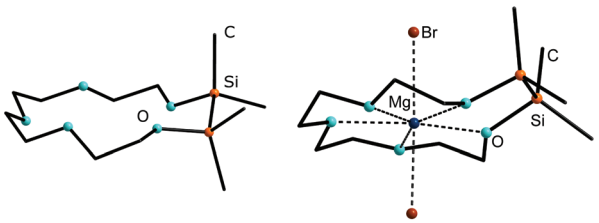

ΔE = -217,36 kJ/mol

1 + [Mg([15]crown-5)Br_2] ⟶ [$MgBr_2$@**1**] (**3**) + [15]crown-5

Scheme 3 Optimized structures of **1** (left) and **3** (right) and relative energies of the cation exchange from [15]crown-5 to 1,2-disila[15]crown-5 (**1**). Calculations performed at the def2-TZVP level of theory. For XYZ-Data and related structures see ESI.†

experimental data such as dynamic ^{1}H NMR spectroscopy. **3** does only barely dissolve in DCM and thus no proton NMR study was possible for this compound.

The heavier calcium cation was incorporated by treating **2** with $Ca(OTf)_2$ (OTf = $F_3CSO_3^-$) in DCM. The resulting coordination compound [Ca(1,2-disila[18]crown-6)OTf_2] (**4**) was obtained as colourless powder. After recrystallization from dichloromethane, single crystals suitable for XRD were obtained in shape of colourless rods. **4** crystallizes in the monoclinic space group $P2_1/n$. This coordination compound shows a mismatch: one of the crown ether oxygen atoms does not participate in the coordination of the central atom. The crown acts as "pseudo-1,2-disila[15]crown-5", so overall five crown ether oxygen atoms together with the two triflate groups coordinate to the calcium cation giving a total coordination number of seven (Fig. 2). The O4–Ca1 atomic distance is 321.4(1) pm. The distorted O7–Ca1–O10 bond angle of 163.0(1)° is a result of the repulsion between O4 and one of the triflate groups.

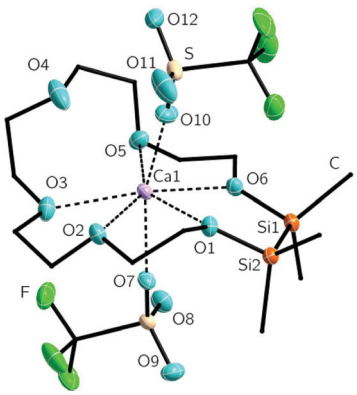

Fig. 2 Molecular structure of **4** in the crystal. Thermal ellipsoids represent a probability level of 50%. Hydrogen atoms are omitted for clarity. Selected bond lengths [pm]: O1–Ca1 244.9(1), O(2)–Ca(1) 245.8(1), O(3)–Ca(1) 247.9(1), O4···Ca1 321.4(1), O5–Ca1 243.6(1), O(6)–Ca1 247.5(1), O(7)–Ca(1) 234.8(1), O(10)–Ca(1) 230.2(2), Si(1)–O(6) 169.6(1), Si(2)–O(1) 169.1(1). Selected bond angles [°]: O1–Ca1–O6 76.1(1), O7–Ca1–O1 85.5(1), O7–Ca1–O2 84.6(1), O7–Ca1–O3 78.3(1), O7–Ca1–O5 99.4(1), O7–Ca1–O6 81.6(1), O7–Ca1–O10 63.0(1).

Hence this angle is slightly smaller than the expected 180° angle which is found in $[Ca(CH_3CH_2OH)_4OTf_2]$.[23]

The O7–Ca1–O(1,2,3,5,6) bond angles differ from 78.3(1) to 99.41(1)° leading to a distorted arrangement of the crown ether oxygen atoms around the calcium cation. The mismatch is obviously caused by the small ion diameter of Ca^{2+}, which is 200 pm, and the enlarged cavity of the ligand **2** compared to [18]crown-6.[24] The coordination pattern of **4** is known for different crown ether complexes.[22,25] However, no mismatched calcium complexes of [18]crown-6 are known to date. Due to the mismatch, the O_{crown}–Ca bond lengths in **4** are slightly shorter than those of complexes of [18]crown-6 and close to [15]crown-5 complexes of calcium (see Table 1). In case of this mismatched crown ether complex, we observed a significantly lower complexation ability of **2** in comparison to [18]crown-6 which was confirmed by means of dynamic ^{1}H NMR spectroscopy (see Scheme 4). An equimolar reaction of **2**, [18]crown-6 and $Ca(OTf)_2$ was carried out. The percentage of coordinated and free ligand was calculated from the average chemical shifts in the mixture according to[36]

$$\delta_{average} = (n_{coordinated}\delta_{coordinated} + n_{noncoordinated}\delta_{noncoordinated})/n_{total}$$

Chemical shifts of compound **4** are significantly high-field shifted in the 1 : 1 mixture of **4** and [18]crown-6, whereas the singlet of [18]crown-6 is significantly down-field shifted (see Scheme 4, spectrum c). As calculated with the above given equation, the ratio of **4** to [Ca([18]crown-6)OTf_2] is 14 : 86. This result is contradicted to experimental data[19] which was observed

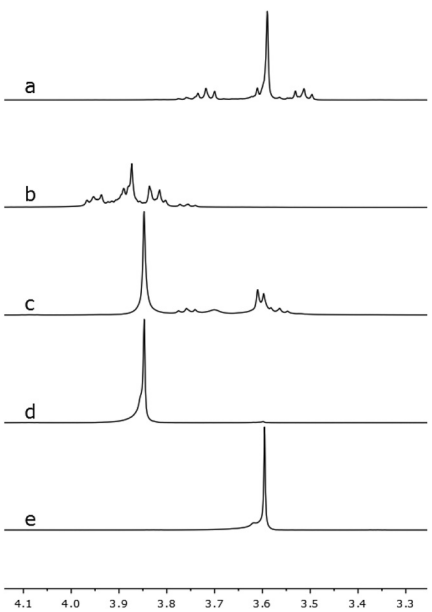

Scheme 4 Segments of 300 MHz ^{1}H NMR Spectra in CD_2Cl_2 of (a) 1,2-disila[18]crown-6, (b) [Ca(1,2-disila[18]crown-6)$(OTf)_2$] (c) [18]crown-6/1,2-disila[18]crown-6/$Ca(OTf)_2$ ratio 1 : 1 : 1 (d) [Ca([18]crown-6)OTf_2] and (e) [18]crown-6.

for the system 1,2,7,8-tetrasila[12]crown-4/$LiPF_6$/[12]crown-4 but attention should be paid to the enlarged cavity size of **2**.

As reported for different supramolecules, the coordination ability of such compounds highly depends on the characteristics of the host-molecule. Especially the size complementarity between cation and host cavity influences the magnitude of the binding constant.[37] The molecular structure of [Ca([18]crown-6)$(OTf)_2(H_2O)$] reveals that [18]crown-6 enables all six oxygen atoms for the coordination to the metal ion rather than only five as in **4**.[30] This is presumably the key advantage of [18]crown-6 over the corresponding disila crown ether **2**.

The halide complex [Sr(1,2-disila[18]crown-6)I_2] (**5**) was synthesized by reaction of **2** with SrI_2 in trifluorotoluene. After recrystallization, **5** was obtained as colourless blocks which were suitable for XRD. **5** crystallizes in the monoclinic space group *C*2/*c* with one solvent molecule DCM. In contrast to **4**, all crown ether oxygen atoms are coordinating to the larger strontium cation (Fig. 3). With two additional iodine atoms, the strontium cation has a coordination number of eight. No crown ether complex of the halide salt SrI_2 is known to date. Actually, different approaches to obtain crown ether complexes of strontium halides yielded [Sr([12]crown-4)$(H_2O)_3$Br]Br or [Sr([18]crown-6)$(H_2O)_3$]X_2 (X = Cl^-, Br^-). Therein no or no more than one halide anion is placed in the coordination sphere of the metal ion.[38,39] Having an ion diameter of 236 pm, the strontium cation is still too small for the hole diameter of **2**.[24] The twisted arrangement of the ligand enables all oxygen atoms to participate in the coordination. The O–Sr1–I1 bond angles differ from 86.1(1) to 96.9(1)° stronger than for example the O–Mg1–Br1 bond angles in **3**. In addition, the $Sr(OSiMe_2)_2$ fragment shows an envelope conformation where the disilane-unit is buckling with Sr–O–O–Si torsion angles of 151.0(1) and 146.8(1)°. The methyl groups are again in an almost eclipsed arrangement with C–Si–Si–C torsion angles of 5.1(1) and 6.2(1)°. The I1–Sr1–I2 bond angle of 177.4(1)° is very close to 180° showing a well-nigh linear coordination of the SrI_2-fragment, which is also observed for [Sr$(DME)_2(THF)I_2$] (DME = 1,2-dimethoxyethane), whose I–Sr–I bond angle is 178.6(1)°.[40]

With bond lengths of 320.1(1) and 320.5(1) pm, the Sr–I bonds are similar to those of different ether adducts such as for example [Sr$(DME)_3I_2$], [Sr$(diglyme)_2I_2$] (diglyme = bis(2-methoxyethyl)ether) or [Sr$(DME)_2(THF)I_2$].[40] Again all carbon substituted oxygen atoms show almost the same bond lengths to the metal ion as the half carbon and half silicon affected oxygen atoms (270.0(2) to 277.7(2) pm). However, the O6–Sr1 bond is the longest one, but should be considered with respect to the twisting of the crown ether. The $Sr–O_{crown}$ bonds of [Sr([18]crown-6)$(NO_3)_3$] and [Sr([18]crown-6)$(HSO_4)_2$] are marginally shorter.[27,32] The cationic crown compounds $[Sr([18]crown-6)(hmpa)_2]^{2+}$ (hmpa = hexamethylphosphoramide) and $[Sr([18]crown-6)L_3]^{2+}$ (L = H_2O, CH_3CN) show notably smaller $Sr–O_{crown}$ bond lengths (see also Table 1).[33,34,39]

Finally, the heaviest non-radioactive alkaline earth metal was incorporated into the macrocycle by treating **2** with $Ba(OTf)_2$ in DCM. After recrystallization, [Ba(1,2-disila[18]crown-6)OTf_2] (**6**) crystallizes in the triclinic space group $P\bar{1}$ with two independent molecules within the asymmetric unit. The metal ion is coordinated by all of the crown ether oxygen atoms as well as by the two triflate groups. One triflate group is coordinating as bidentate ligand giving the barium cation a total coordination number of nine (Fig. 4). With its ion diameter of 270 pm the barium cation is larger than the strontium cation, but the crown is still twisting as shown by the O5–Ba1–O10 and O6–Ba1–O10 bond angles, which are 78.1(1) and 77.4(1)°

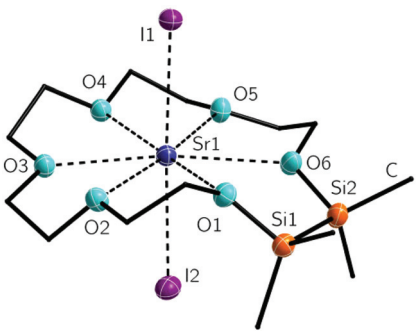

Fig. 3 Molecular structure of **5** in the crystal. Thermal ellipsoids represent a probability level of 50%. Hydrogen atoms and one solvent molecule DCM are omitted for clarity. Selected bond lengths [pm]: O1–Sr1 273.8(1), O2–Sr1 273.8(1), O3–Sr1 270.0(2), O4–Sr1 273.5(1), O5–Sr1 271.0(1), O6–Sr1 277.7(2), I1–Sr1 320.1(1), I2–Sr1 320.5(1), Si1–O1 167.6(2), Si2–O6 167.7(2), Si1–Si2 233.4(1). Selected bond angles [°]: O1–Sr1–I1 88.0(1), O2–Sr1–I1 93.2(1), O3–Sr1–I1 96.9(1), O4–Sr1–I1 87.0(1), O5–Sr1–I1 86.1(1), O6–Sr1–I1 93.2(1), I1–Sr1–I2 177.4(1), Sr1–O1–O6–Si2 151.0(1), Sr1–O6–O1–Si1 146.8(1).

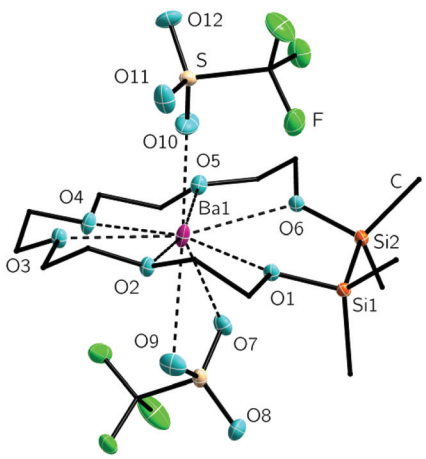

Fig. 4 Molecular structure of **6** in the crystal. Thermal ellipsoids represent a probability level of 50%. Hydrogen and disordered atoms with lower occupancy are omitted for clarity. Only one of two independent molecules per asymmetric unit is shown. Selected bond lengths [pm]: O1–Ba1 283.8(1), O2–Ba1 277.5(1), O3–Ba1 285.3(1), O4–Ba(1) 285.9, O5–Ba1 284.0(1), O6–Ba1 279.8(1), O7–Ba1 292.1(1), O9–Ba1 288.7, O10–Ba1 253.9(3), Si1–O1 168.5(1), Si2–O6 168.1(1), Si1–Si2 234.6(1). Selected bond angles [°]: O1–Ba1–O6 69.3(1), O1–Ba1–O4 168.6(1), O2–Ba1–O5 167.3(1), O3–Ba1–O6 166.0(1), Ba1–O1–O6–Si2 157.6(1), Ba1–O6–O1–Si1 156.5(1).

Table 2 Selected bond lengths [pm] for compounds **6**, **8** and their related crown ether complexes

Compound	O_{crown}–Ba [pm]	CN[a]	Ref.
$[Ba([18]crown-6)(hmpa)_2][BPh_4]_2$	277.2(2)–281.3(2)	8	34
$[Ba([18]crown-6)(hmpa)_2][SnPh_3]$	277(1)–280(1)	8	35
$[Ba([18]crown-6)(HCPh_2)_2]$	275.0(2)–280.2(3)	8	41
$[Ba([18]crown-6)(PPh)_2]$	271.7(2)–280.7(2)	8	42
$[Ba([18]crown-6)(hmpa)_2](SeMes^*)_2$ [b]	276.7(3)–280.3(2)	8	43
6	277.5(1)–285.9(1)	9	[c]
8	277.5(2)–289.9(2)	9	[c]
$[Ba([18]crown-6)(NCS)_2(H_2O)]$	280.8(6)–287.5(5)	9	44
$[Ba([18]crown-6)\{O_2P(OnBu)_2\}(H_2O)]$	281(2)–290(2)	9	45
$[Ba([18]crown-6)(O_2CCF_3)_2(py)]$	282.0(5)–284.5(7)	10	46
$[Ba([18]crown-6)(pta)_2]$ [d]	278.6(3)–283.1(3)	10	47
$[Ba(DB[18]crown-6)(pta)_2]$ [e]	292.9(4)–317.1(4)	10	47
$[Ba([18]crown-6)(H_2O)_3Cl]Cl$	277.0(2)–285.4(1)	10	48
$[Ba([18]crown-6)(O_2CCH_3)_2]$	275.3(2)–283.5(2)	10	49
$[Ba([18]crown-6)(NO_3)_2H_2O]$	283(1)–290.8(8)	11	27

[a] Coordination number. [b] Mes* = 2,4,6-$tBu_3C_6H_2$. [c] This work. [d] pta = 1,1,1-trifluoro-5,5-dimethylhexane-2,4-dione. [e] DB = dibenzo.

respectively.[24] The O1–4–Ba1–O10 angles are much closer to 90°. The O_{crown}–Ba bond lengths of 277.5(1) to 285.9(1) pm are in accordance with those of different [18]crown-6 complexes with barium. Nevertheless these distances are dependent on several factors such as coordination number, donor strength and the sterically demand of coligands (see Table 2).

Similar to the compounds **3–5**, the silicon bonded oxygen atoms do not differ significantly concerning the oxygen metal distance in comparison to the fully carbon substituted oxygen atoms. Again an eclipsed arrangement of the methyl groups at the silicon atoms is found. With 2.3(1) and 2.7(1)° the C–Si–Si–C torsion angles are even smaller. The monodentate coordinating triflate group binding to the metal ion has a O(10)–Ba1 bond length of 253.9(3) pm. The chelating triflate group has significantly longer bond lengths of 288.7(1) and 292.1(1) pm. This is very similar to the trifluoroacetate groups in the complex $[Ba(O_2CCF_3)_2([18]crown-6)(py)]$ (py = pyridine). The trifluoroacetate group, which acts as monodentate ligand, has O–Ba bond length of 263.1(9) pm. The chelating one has a bond length of 287.6(1) pm.[46] To what extend these complexes are affected by negative hyperconjugation is still a matter of interest. We therefore claimed to crystallize a free ligand which can be compared to coordination compounds and started to prepare the heavier benzylic crown ether 1,2-disila-benzo[18]crown-6 (**7**). The organic fragment of 1,2-disila-benzo[18]crown-6 was synthesized by reaction of catechol and 2-(2-chlorethoxy)ethanol.[50] Subsequent addition of 1,2-dichloro-1,1,2,2-tetramethyldisilane yielded compound **7** (Scheme 5). However, **7** was obtained as a viscous oil, so no crystal structure could be obtained. An investigation regarding the coordination ability of **7** was still interesting because the benzylic unit as well as the Si_2Me_4 fragment are considerably unpliable. Coordination chemistry was performed by reaction of **7** with $Ba(OTf)_2$, yielding $[Ba(1,2\text{-disila-Benzo}[18]crown\text{-}6)OTf_2]$ (**8**), which crystallizes in the orthorhombic space group $P2_12_12_1$ (Fig. 5).

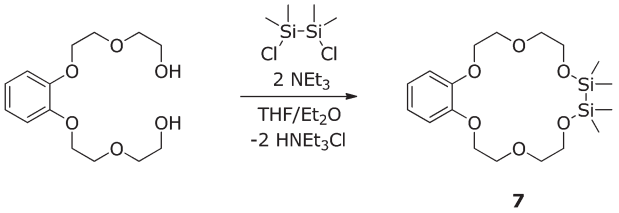

7

Scheme 5 Synthesis of 1,2-disila-benzo[18]crown-6.

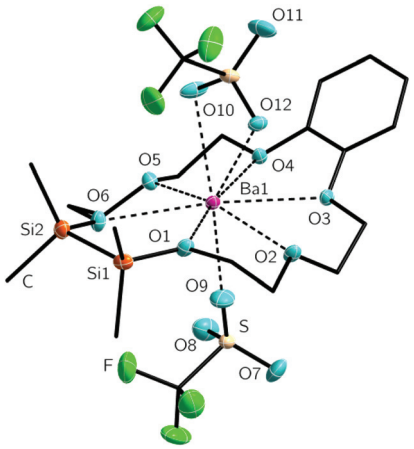

Fig. 5 Molecular structure of **8** in the crystal. Thermal ellipsoids represent a probability level of 50%. Hydrogen and disordered atoms with lower occupancy are omitted for clarity. Selected bond lengths [pm]: O1–Ba1 279.6(2), O2–Ba1 278.2(2), O3–Ba1 289.9(2), O4–Ba(1) 284.9(1), O5–Ba1 277.5(2), O6–Ba1 286.6(2), O9–Ba1 263.0(7), O10–Ba1 282.8(4), O12–Ba1 279.9(1), Si1–O1 167.8(2), Si2–O6 167.5(2), Si1–Si2 233.9(1). Selected bond angles [°]: O1–Ba1–O6 70.8(1), O1–Ba1–O4 170.0(1), O2–Ba1–O5 157.0(1), O3–Ba1–O6 166.3(1).

As previously shown for **6**, the metal ion in **8** is coordinated by all of the crown ether oxygen atoms as well as the two triflate groups. The barium ion is only slightly shifted out of the center of the crown ether. The transannular angles of 157.0(1) to 170.0(1)° are close to 180°, so the barium cation fits well into the cavity of **7**.

In contrast to **6**, the twisting of the crown is absent. The crown ether is rather bent with the benzylic as well as the disilane unit buckling to one side. With 277.5(2)–289.9(2) pm, the O_{crown}–Ba distances have almost the same lengths as in **6**. So have those of related compounds (see Table 2). Similar to **6**, one triflate group is chelating, the other one bonds to the metal ion only by a single oxygen atom. In comparison to O9, whose atomic distance to the metal ion is 263.0(7) pm, the chelating oxygen atoms of the triflate group have O10–Ba1 and O12–Ba1 atomic distances of 282.8(4) and 279.1(6) pm, respectively. The methyl groups of the $SiMe_2$ units are only slightly contorted to each other and show torsion angles of 16.8(1) and 18.3(1)°.

According to recently published work another key role in understanding the complexation ability of silicon based crown ethers analogues is the repulsion between the positively

charged metal ion and the positively polarized silicon atoms.[14] The use of Si_2Me_4 rather than one $SiMe_2$ allows lower repulsion, which can be seen in the average Si–M distances. This might also be an explanation for the higher complexation ability of these hybrid disila-crown ethers in comparison to cyclosiloxanes which we reported before. Further calculations would be helpful to quantify though. Experimental data of metal complexes with disila units, however, features longer average Si–M distances than the sila units in siloxanes. While [Li(1,2-disila[12]crown-4)OTf] has average M–Si distances of 321.6 pm they are shortened to 272–275 pm in the cyclosiloxane complexes $[Li(D_6)Al_F]$ and $[Li(D_6)Al_{PhF}]$ (Al_{PhF} = $[Al\{OC(CF_3)_2Ph\}_4]^-$).[2,19] [K(1,2-disila[18]crown-6)PF_6] has Si–M average distances of 392.4(1) pm.[19] $[K(D_7)]^+$ has average distances of 358–365 pm, so these are shortened as well.[4,21] Analogous observations were made in the comparison of alkaline earth metal complexes reported in this work like **5** and **6** with siloxane complexes such as $[Sr(NBN\text{-}SiMe_2OSiMe_2O)THF]_2$ or $[Ba(THF)_6(dmpz)_8\{(OSiMe_2)O\}_2]$ (dmpz = 3,5-dimethylpyrazolate).[51,52] Still no complexes of common cyclosiloxanes and alkaline earth metal salts are known today, so the reported complexes in this work are the first crown-type structures containing an alkaline earth metal as well as ligands bearing Si–O donors.

Conclusions

In a recent work, we described the synthesis of hybrid disila-crown ethers of the type 1,2-disila[3*n*]crown-*n* (**1**: *n* = 5, **2**: *n* = 6) and the formation of alkaline metal complexes.[19] Within this study, we reported the synthesis of 1,2-disila-benzo[18]crown-6 (**7**) using similar conditions.

By equimolar reaction of alkaline earth metal salts with the disila-crown ethers **1**, **2** and **7**, we obtained the alkaline earth metal complexes **3–6** and **8**. The structures of all coordination compounds were determined *via* X-ray crystallographic studies. The O_{crown}–M bond lengths indicate that all carbon substituted oxygen atoms show almost the same bond lengths to the metal ion as the half carbon and half silicon affected oxygen atoms, so that on a structural level no reduced complexation ability of these O–Si_2Me_4–O fragments can be observed. The variation of ion diameter and cavity diameter of the crown then gives interesting coordination patterns: in compound **4**, the cavity diameter of **2** is too large for the calcium ion resulting in a mismatch structure. This structure reveals that it's not inevitably the silicon affected oxygen atom which does not participate in the coordination but according to proton NMR-studies, the complexation ability of 1,2-disila[18]crown-6 (**2**) was determined to be significantly lower than those of [18]crown-6. The size complementarity between cation and host cavity significantly influences the complex stabilities.

Beside the triflate complexes **4**, **6** and **8**, we also obtained complexes with strongly coordinating anions such as Br^- or I^- (compound **3** and **5**). These results show a better coordination ability of disila-bridged donor atoms in comparison to R_2Si bridges, which results from longer Si–M distance within the metal complexes and a reduced cyclic stress. Furthermore DFT calculations (BP86 functional and def2-TZVP basis set) revealed that the coordination ability of 1,2-disila[15]crown-5 (**1**) towards magnesium bromide is considerably higher compared to [15]crown-5. Nonetheless, all disila-substituted crown ether oxygen atoms of the type SiSi–O–SiSi would still be useful to give more meaningful results in how far disila-affected crown ethers can challenge organic crown compounds. Most recent work hints a considerably higher complexation ability of the partially silicon substituted crown ether 1,2,4,5-tetrasila[12]crown-4 towards Li^+ than [12]crown-4.[53] Thus, further investigations for this kind of crown ethers and a stepwise synthesis of a fully silicon substituted crown ether are intended for the future.

Experimental section

General

All working procedures were carried out with rigorous exclusion of oxygen and moisture using Schlenk techniques under inert gas atmosphere. Solvents were dried and freshly distilled before use. Compounds **1**, **2** and the organic fragment of **7** were synthesized using methods described in literature.[19,50] Alkaline earth metal salts were stored and handled under argon atmosphere using a glovebox. NMR spectra were recorded on a Bruker AV III HD 300 MHz or AV III 500 MHz. Infrared (IR) spectra of the respective samples were measured using attenuated total reflectance (ATR) mode on a Bruker Model Alpha FT-IR. MS-spectrometry was measured on JEOL AccuTOF-GC (LIFDI) or LTQ-FT (ESI). Elemental analysis was performed on a Vario MicroCube. Fluorine-containing compounds led to ongoing damage of the elemental analyser and were not measured.

Synthesis of [Mg(1,2-disila[15]crown-5)Br_2] (3). 0.244 g 1,2-disila[15]crown-5 (0.79 mmol) are dissolved in 15 mL trifluorotoluene, and 0.146 g (0.79 mmol) $MgBr_2$ are added. The suspension is stirred for four days and then filtered. The residue is washed with 4 mL DCM, and the filtrate is freed of the solvent. The resulting solid is washed with three portions of 5 mL *n*-pentane, dissolved in 2 mL DCM and layered with 10 mL *n*-pentane. After two days, **3** is obtained as colourless blocks (0.12 g, 30%). Elemental Analysis [%] found (calc.): C 28.83 (29.26) H 6.18 (5.73).

^{1}H NMR: (300 MHz, CD_2Cl_2) δ = 0.44 (s, 12H, Si(CH_3)$_2$), 3.77–3.80 (m, 4H, CH_2), 3.86 (s, 8H, CH_2), 3.95–3.98 (m, 4H, CH_2) ppm; $^{13}C\{^1H\}$ NMR: (75 MHz, CD_2Cl_2) δ = −0.8 (s, Si(CH_3)$_2$), 61.8 (s, CH_2), 68.1 (s, CH_2), 68.5 (s, CH_2), 69.9 (s, CH_2) ppm; $^{29}Si\{^1H\}$ NMR: (99 MHz, CD_2Cl_2) δ = 18.0 (s, *Si*(CH_3)$_2$) ppm; MS: LIFDI(+) *m*/*z* (%): 411.051 $[M - Br]^+$ (83); IR (cm^{-1}): 2948 (m), 2884 (w), 1634 (w), 1467 (m), 1345 (w), 1297 (w), 1243 (m), 1084 (s), 1058 (s), 1046 (s), 959 (s), 922 (m), 896 (m), 824 (m), 803 (m), 774 (w), 730 (s), 696 (w), 639 (w), 568 (w).

Synthesis of [Ca(1,2-disila[18]crown-6)OTf_2] (4). 0.192 g 1,2-disila[18]crown-6 (0.79 mmol) are dissolved in 15 mL DCM,

and 0.146 g (0.79 mmol) $CaOTf_2$ are added. The suspension is stirred vigorously overnight and then filtered. The residue is washed with 2 mL DCM and the filtrate is freed of the solvent. The resulting solid is washed with three portions of 5 mL *n*-pentane, dissolved in 5 mL DCM and layered with 10 mL *n*-pentane. After two days, **4** is obtained as colourless rods (0.187 g, 39%).

^{1}H NMR: (300 MHz, CD_2Cl_2) δ = 0.41 (s, 12H, Si(CH_3)$_2$), 3.80–3.84 (m, 4H, CH_2), 3.87–3.89 (m, 12H, CH_2), 3.94–3.97 (m, 4H, CH_2) ppm; ^{13}C{^{1}H} NMR: (75 MHz, CD_2Cl_2) δ = −0.9 (s, Si(*C*H$_3$)$_2$), 62.9 (s, *C*H$_2$), 69.7 (s, *C*H$_2$), 70.3 (s, *C*H$_2$), 70.7 (s, *C*H$_2$), 72.7 (s, *C*H$_2$), 120.7 (q, $^1J_{CF}$ = 318 Hz, *C*F$_3$) ppm; ^{29}Si{^{1}H} NMR: (99 MHz, CD_2Cl_2) δ = 19.7 (s, *Si*(CH$_3$)$_2$) ppm; ^{19}F NMR: (282 MHz, CD_2Cl_2) δ = −79.3 (s, C*F*$_3$) ppm; MS LIFDI(+) *m*/*z* (%): 375.165 [1,2-disila[18]crown-6 + Na]$^+$ (100), 541.088 [M − OTf]$^+$ (40); IR (cm^{-1}): 2954 (w), 2887 (w), 1471 (w), 1357 (w), 1305 (s), 1240 (s), 1219 (s), 1164 (s), 1059 (s), 1028 (s), 935 (s), 868 (m), 838 (s), 817 (s), 795 (s), 775 (s), 760 (s), 726 (s), 634 (s), 579 (m), 514 (s), 460 (w).

Synthesis of [Sr(1,2-disila[18]crown-6)I$_2$] (5). 0.355 g 1,2-disila[18]crown-6 (1.00 mmol) are dissolved in 20 mL trifluorotoluene, and 0.343 g (0.79 mmol) SrI_2 are added. The suspension is stirred under exclusion of light for 12 h and then filtered. The residue is washed with 2 mL DCM, and the filtrate is freed of the solvent. The resulting solid is washed with three portions of 5 mL *n*-pentane, dissolved in 3 mL DCM and layered with 15 mL *n*-pentane. After two days, **5** is obtained as colourless plates (0.227 g, 33%). Elemental Analysis [%] found (calc.): C 24.23 (23.96) H 5.05 (4.65).

^{1}H NMR: (300 MHz, CD_2Cl_2) δ = 0.46 (s, 12H, Si(CH_3)$_2$), 3.81–3.84 (m, 4H, CH_2), 3.90 (s, 4H, CH_2), 3.91–3.96 (m, 8H, CH_2), 4.05–4.08 (m, 4H, CH_2) ppm; ^{13}C{^{1}H} NMR: (75 MHz, CD_2Cl_2) δ = 0.0 (s, Si(*C*H$_3$)$_2$), 63.1 (s, *C*H$_2$), 70.4 (s, *C*H$_2$), 70.5 (s, *C*H$_2$), 70.5 (s, *C*H$_2$), 73.0 (s, *C*H$_2$) ppm; ^{29}Si{^{1}H} NMR: (99 MHz, CD_2Cl_2) δ = 18.2 (s, *Si*(Me)$_2$) ppm. MS: LIFDI(+) *m*/*z* (%): 566.984 [M − I]$^+$ (100); IR (cm^{-1}): 2943 (w), 2881 (w), 1457 (w), 1353 (w), 1320 (w), 1245 (m), 1082 (s), 1039 (s), 972 (s), 957 (s), 930 (s), 919 (s), 862 (s), 841 (s), 823 (s), 797 (s). 769 (s), 729 (s), 696 (m), 657 (w), 628 (m), 532 (w), 461 (w).

Synthesis of [Ba(1,2-disila[18]crown-6)OTf$_2$] (6). 0.100 g 1,2-disila[18]crown-6 (0.28 mmol) are dissolved in 15 mL DCM, and 0.124 g (0.28 mmol) $BaOTf_2$ are added. The suspension is stirred overnight and then filtered. The residue is washed with 2 mL DCM and the filtrate is freed of the solvent. The resulting solid is washed with three portions of 5 mL *n*-pentane, dissolved in 4 mL DCM and layered with 10 mL *n*-pentane. After two days, **6** is obtained as colourless blocks (0.103 g, 38%).

^{1}H NMR: (300 MHz, CD_2Cl_2) δ = 0.36 (s, 12H, Si(CH_3)$_2$), 3.68–3.70 (m, 4H, CH_2), 3.78 (s, 12H, CH_2), 3.86–3.88 (m, 4H, CH_2) ppm; ^{13}C{^{1}H} NMR: (75 MHz, CD_2Cl_2) δ = −0.9 (s, Si(*C*H$_3$)$_2$), 63.6 (s, *C*H$_2$), 70.7 (s, *C*H$_2$), 70.9 (s, *C*H$_2$), 71.3 (s, *C*H$_2$), 73.2 (s, *C*H$_2$), 120.9 (q, $^1J_{CF}$ = 321 Hz, *C*F$_3$) ppm; ^{19}F NMR: (282 MHz, CD_2Cl_2) δ = −79.1 (s, C*F*$_3$) ppm; ^{29}Si{^{1}H} NMR: (99 MHz, CD_2Cl_2) δ = 17.6 (s, *Si*(CH$_3$)$_2$) ppm; MS ESI(+) *m*/*z* (%): 639.031 [M − OTf]$^+$ (100); IR (cm^{-1}): 2951 (w), 2925 (w), 2888 (w), 1475 (w), 1456 (w), 1353 (w), 1296 (s), 1242 (s), 1223 (s), 1164 (s), 1123 (s), 1105 (s), 1083 (s), 1074 (s), 1024 (s), 964 (s), 952 (s), 917 (w), 896 (w), 873 (m), 864 (s), 842 (s), 821 (s), 799 (m), 774 (s), 759 (m), 736 (s), 719 (m), 698 (w), 631 (s), 580 (s), 574 (s), 540 (s), 514 (s), 456 (w).

Synthesis of 1,2-disila-benzo[18]crown-6 (7). 0.73 g of 1,2-bis(5-hydroxy-3-oxa-1-pentyloxy)benzene (2.55 mmol) and 0.49 mL 1,2-dichloro-1,1,2,2-tetramethyldisilane (2.55 mmol) are dissolved in 50 mL of THF each and added dropwise into a stirred solution of 100 mL THF, 20 mL Et_2O and 0.7 mL triethylamine (5.1 mmol) simultaneously over a period of 90 min. After stirring the solution overnight, the solvent is removed under reduced pressure. The residue is resolved in 20 mL toluene and filtered. The solvent is removed again and 4 mL acetonitrile is added. The crude product is gently washed and the solution is decanted. The solvent is yet again removed under reduced pressure and the resulting oil is dried *in vacuo* at 1×10^{-3} mbar for several hours. The crown ether is obtained as colourless, slightly yellow oil (0.77 g, 75%).

^{1}H NMR: (300 MHz, CD_3CN) δ = 0.21 (s, 12H, Si(CH_3)$_2$), 3.60–3.63 (m, 4H, CH_2), 3.75–3.80 (m, 8H, CH_2), 4.08–4.11 (m, 4H, CH_2), 6.87–6.98 (m, 4H, CH_{AR}) ppm; ^{13}C{^{1}H} NMR: (75 MHz, CD_3CN) δ = −0.29 (s, Si(*C*H$_3$)$_2$), 63.9 (s, *C*H$_2$), 69.8 (s, *C*H$_2$), 70.4 (s, *C*H$_2$), 73.6 (s, *C*H$_2$), 114.7 (s, *C*H$_2$), 122.2 (s, *C*H$_{Ar}$), 149.8 (s, C_{qAr}) ppm. ^{29}Si{^{1}H} NMR: (99 MHz, CD_3CN): δ = 11.0 (s, *Si*(CH$_3$)$_2$) ppm; MS (LIFDI+) *m*/*z* (%): 400.17443 [M]$^+$ (20); IR (cm^{-1}): 2947 (m), 2868 (m), 1593 (m), 1501 (s), 1453 (m), 1396 (w), 1356 (w), 1328 (w), 1248 (s), 1219 (s), 1125 (s), 1088 (s), 1051 (s), 943 (s), 826 (s), 789 (s), 763 (s), 740 (s), 682 (w), 658 (m), 630 (w), 481 (w).

Synthesis of [Ba(1,2-disila-benzo[18]crown-6)OTf$_2$] (8). 0.164 g 1,2-disila-benzo[18]crown-6 (0.41 mmol) are dissolved in 15 mL DCM, and 0.178 g (0.28 mmol) $BaOTf_2$ are added. The suspension is stirred for 6 h and then filtered. The residue is washed with 2 mL DCM and the filtrate is freed of the solvent. The resulting solid is washed with four portions of 10 mL *n*-pentane, dissolved in 4 mL DCM and layered with 15 mL *n*-pentane. After two days, **8** is obtained as colourless blocks (0.120 g, 35%).

^{1}H NMR: (300 MHz, CD_2Cl_2) δ = 0.36 (s, 12H, Si(CH_3)$_2$), 3.81–3.88 (m, 8H, CH_2), 4.03–4.06 (m, 4H, CH_2), 4.24–4.27 (m, 4H, CH_2), 6.93–7.03 (m, 4H, CH_{AR}) ppm; ^{13}C{^{1}H} NMR: (75 MHz, CD_2Cl_2) δ = −0.9 (s, Si(*C*H$_3$)$_2$), 63.4 (s, *C*H$_2$), 68.4 (s, *C*H$_2$), 69.6 (s, *C*H$_2$), 73.4 (s, *C*H$_2$), 112.3 (s, *C*H$_{AR}$), 120.8 (q, $^1J_{CF}$ = 319 Hz, *C*F$_3$), 122.8 (s, *C*H$_{Ar}$), 146.9 (s, $C_{q,Ar}$) ppm; ^{19}F NMR: (282 MHz, CD_2Cl_2) δ = −78.7 (s, C*F*$_3$) ppm; ^{29}Si{^{1}H} NMR: (99 MHz, CD_2Cl_2) δ = 17.7 (s, *Si*(CH$_3$)$_2$) ppm; MS LIFDI (+) *m*/*z* (%): 687.031 [M − OTf]$^+$ (100), 1523.014 [2M − OTf]$^+$ (100); IR (cm^{-1}): 2945 (w), 2885 (w), 1596 (w), 1506 (s), 1477 (m), 1456 (w), 1357 (s), 1300 (s), 1240 (s), 1220 (s), 1171 (s), 1115 (s), 1063 (s), 1034 (s), 1023 (s), 961 (s), 941 (s), 914 (s), 865 (m), 852 (s), 837 (s), 819 (s), 795 (s), 772 (s), 756 (s), 737 (s), 634 (s), 604 (m), 583 (m), 573 (m), 528 (m), 513 (s), 454 (w).

Computational details

Calculations were performed with the program system TURBOMOLE V7.0.1.[54] The resolution of identity (RI) approxi-

mation, dispersion corrections, and the conductor-like screening model (COSMO) were applied throughout, the latter with default settings. For all calculations, the BP86 functional was chosen, utilizing a def2-TZVP basis set.[55]

Crystal structures

Single crystal X-ray diffraction was carried out using Bruker D8 Quest (**3**, **6**, **8**) or IPDS 2 diffractometer (**4**, **5**) at 100–110 K with MoK_α radiation and X-ray optics or graphite monochromatization, respectively (λ = 0.71073). The structures were solved by direct methods and refinement with full-matrix-least-squares against F^2 using SHELXT- and SHELXL-2015 on OLEX2 platform.[56–58] Triflate groups were refined with help of DSR.[59] Crystallographic data for compounds **3–6** and **8** are denoted as follows: CCDC No. 1497469 (**3**), 1497467 (**4**), 1497468 (**5·DCM**), 1497471 (**6**) and 1497470 (**8**).

Crystal data of 3. $C_{12}H_{28}Br_2MgO_5Si_2$, orthorhombic, *Pbca*, Z = 8, 100 K, a = 10.8339(6) Å, b = 14.1089(7) Å, c = 27.7505(14) Å, V = 4241.8(4) Å^3, ρ = 1.543 g cm^{-3}, multiscan absorption correction using SADABS-2014,[60] μ = 3.980 mm^{-1}, T_{min}, T_{max} = 0.622, 0.745, 2Θ range 4.77–50.54°, reflections measured 22 357, independent reflections 3841 [R(int) = 0.0724], 203 parameters, R-index [$I \geq 2\sigma(I)$] 0.0322, wR_2 (all data) 0.0553, GOOF 1.023, $\Delta\rho_{max}$, $\Delta\rho_{min}$ 0.40/−0.41 e Å^3.

Crystal data of 4. $C_{16}H_{32}CaF_6O_{12}S_2Si_2$, monoclinic, $P2_1/n$, Z = 4, 100 K, a = 8.9460(18) Å, b = 34.272(7) Å, c = 9.6976(19) Å, β = 103.04°, V = 2896.6(11) Å^3, ρ = 1.584 g cm^{-3}, numerical absorption correction using X-AREA and X-RED32,[61] μ = 0.535 mm^{-1}, T_{min}, T_{max} = 0.874, 0.951, 2Θ range 4.48–49.62°, reflections measured 13 664, independent reflections 4991 [R(int) = 0.0780], 358 parameters, R-index [$I \geq 2\sigma(I)$] 0.0408, wR_2 (all data) 0.1089, GOOF 1.008, $\Delta\rho_{max}$, $\Delta\rho_{min}$ 0.73/–0.67 e Å^3.

Crystal data of 5·DCM. $C_{15}H_{34}Cl_2I_2O_6Si_2Sr$, monoclinic, $C2/c$, Z = 8, 100 K, a = 14.037(3) Å, b = 10.896(2) Å, c = 37.359(8) Å, β = 99.19(3)°, V = 5641(2) Å^3, ρ = 1.834 g cm^{-3}, numerical absorption correction using X-AREA and X-RED32,[61] μ = 4.400 mm^{-1}, T_{min}, T_{max} = 0.482, 0.709, 2Θ range 4.756–52.016°, reflections measured 15 303, independent reflections 5516 [R(int) = 0.0290], 257 parameters, R-index [$I \geq 2\sigma(I)$] 0.0191, wR_2 (all data) 0.0360, GOOF 0.800, $\Delta\rho_{max}$, $\Delta\rho_{min}$ 0.60/−0.61 e Å^3.

Crystal data of 6. $C_{16}H_{32}BaF_6O_{12}S_2Si_2$, triclinic, $P\bar{1}$, Z = 4, Z' = 2, 100 K, a = 9.7531(4) Å, b = 17.5485(8) Å, c = 18.5666(8) Å, α = 72.5040(10)°, β = 86.902(2)° γ = 89.5490(10)°, V = 3026.2(2) Å^3, ρ = 1.617 g cm^{-3}, multiscan absorption correction using SADABS-2014,[60] μ = 1.617 mm^{-1}, T_{min}, T_{max} = 0.544, 1.000, 2Θ range 4.518–61.68°, reflections measured 103 763, independent reflections 18 918 [R(int) = 0.0254], 982 parameters, R-index [$I \geq 2\sigma(I)$] 0.0237, wR_2 (all data) 0.0509, GOOF 1.093, $\Delta\rho_{max}$, $\Delta\rho_{min}$ 1.03/−2.70 e Å^3.

Crystal data of 8. $C_{20}H_{32}BaF_6O_{12}S_2Si_2$, orthorhombic, $P2_12_12_1$, Z = 4, 110 K, a = 9.0173(4) Å, b = 10.3761(5) Å, c = 35.6495(16) Å, V = 3335.5(3) Å^3, ρ = 1.665 g cm^{-3}, numerical absorption correction using SADABS-2014,[60] μ = 1.473 mm^{-1}, T_{min}, T_{max} = 0.668, 0.904, 2Θ range 4.542–57.452°, reflections measured 32 181, independent reflections 8616 [R(int) = 0.0346], 525 parameters, R-index [$I \geq 2\sigma(I)$] 0.0274, wR_2 (all data) 0.0481, GOOF 1.037, $\Delta\rho_{max}$, $\Delta\rho_{min}$ 0.59/−0.60 e Å^3, Flack parameter 0.002(6).

Acknowledgements

This work was financially supported by the Deutsche Forschungsgemeinschaft (DFG).

References

1 J. S. Ritch and T. Chivers, *Angew. Chem.*, 2007, **119**, 4694–4697, (*Angew. Chem., Int. Ed.*, 2007, **46**, 4610–4613).
2 A. Decken, J. Passmore and X. Wang, *Angew. Chem.*, 2006, **118**, 2839–2843, (*Angew. Chem., Int. Ed.*, 2006, **45**, 2773–2777).
3 C. von Hänisch, O. Hampe, F. Weigend and S. Stahl, *Angew. Chem.*, 2007, **119**, 4859–4863, (*Angew. Chem., Int. Ed.*, 2007, **46**, 4775–4779).
4 M. R. Churchill, C. H. Lake, S.-H. L. Chao and O. T. Beachley, *J. Chem. Soc., Chem. Commun.*, 1993, **1**, 1577–1578.
5 A. Decken, F. A. LeBlanc, J. Passmore and X. Wang, *Eur. J. Inorg. Chem.*, 2006, 4033–4036.
6 I. Krossing and I. Raabe, *Angew. Chem.*, 2004, **116**, 2116–2142, (*Angew. Chem., Int. Ed.*, 2004, **43**, 2066–2090).
7 R. D. Ernst, A. Glöckner and A. M. Arif, *Z. Kristallogr.*, 2007, **222**, 333–334.
8 J. Passmore and J. M. Rautiainen, *Eur. J. Inorg. Chem.*, 2012, 6002–6010.
9 F. Weinhold and R. West, *Organometallics*, 2011, **30**, 5815–5824.
10 F. Weinhold and R. West, *J. Am. Chem. Soc.*, 2013, **135**, 5762–5767.
11 H. Oberhammer and J. E. Boggs, *J. Am. Chem. Soc.*, 1980, **102**, 7241–7244.
12 R. J. Gillespie and S. A. Johnson, *Inorg. Chem.*, 1997, **36**, 3031–3039.
13 S. Grabowsky, M. F. Hesse, C. Paulmann, P. Luger and J. Beckmann, *Inorg. Chem.*, 2009, **48**, 4384–4393.
14 T. S. Cameron, A. Decken, I. Krossing, J. Passmore, J. M. Rautiainen, X. Wang and X. Zeng, *Inorg. Chem.*, 2013, **52**, 3113–3126.
15 M. Ouchi, Y. Inoue, T. Kanzaki and T. Hakushi, *Bull. Chem. Soc. Jpn.*, 1984, **57**, 887–888.
16 Y. Inoue, M. Ouchi and T. Hakushi, *Bull. Chem. Soc. Jpn.*, 1985, **58**, 525–530.
17 D. J. Harrison, D. R. Edwards, R. McDonald and L. Rosenberg, *Dalton Trans.*, 2008, 3401–3411.
18 M. K. Skjel, A. Y. Houghton, A. E. Kirby, D. J. Harrison, R. McDonald and L. Rosenberg, *Org. Lett.*, 2010, **12**, 376–379.
19 K. Reuter, M. R. Buchner, G. Thiele and C. von Hänisch, *Inorg. Chem.*, 2016, **55**, 4441–4447.

20 M. Stürmann, W. Saak, M. Weidenbruch and K. W. Klinkhammer, *Eur. J. Inorg. Chem.*, 1999, 579–582.
21 C. Eaborn, P. B. Hitchcock, K. Izod and J. D. Smith, *Angew. Chem.*, 1995, **107**, 2936–2937, (*Angew. Chem., Int. Ed. Engl.*, 1996, **34**, 2679–2680).
22 J. L. Atwood, S. G. Bott, C. M. Means, A. W. Coleman, H. Zhang and M. T. May, *Inorg. Chem.*, 1990, **29**, 467–470.
23 M. Barboiu and A. van der Lee, *Acta Crystallogr., Sect. C: Cryst. Struct. Commun.*, 2003, **59**, m366–m368.
24 M. Trömel, *Z. Naturforsch.*, 2000, **55b**, 243–247.
25 S. Chadwick and K. Ruhlandt-Senge, *Chem. – Eur. J.*, 1998, **4**, 1768–1780.
26 S. Chadwick, U. Englich and K. Ruhlandt-Senge, *Inorg. Chem.*, 1999, **38**, 6289–6293.
27 P. C. Junk and J. W. Steed, *J. Chem. Soc., Dalton Trans.*, 1999, 407–414.
28 Y. Y. Wei, B. Tinant, J. P. Declercq, M. Van Meerssche and J. Dale, *Acta Crystallogr., Sect. C: Cryst. Struct. Commun.*, 1988, **44**, 73–77.
29 T. B. Rubtsova, O. K. Kireeva, B. M. Bulychev, N. P. Streltsova, V. K. Belsky and B. P. Tarasov, *Polyhedron*, 1992, **11**, 1929–1938.
30 P. Farina, W. Levason and G. Reid, *Dalton Trans.*, 2013, **42**, 89–99.
31 J. Langer, S. Krieck, R. Fischer, H. Görls and M. Westerhausen, *Z. Anorg. Allg. Chem.*, 2010, **636**, 1190–1198.
32 D. Braga, M. Gandolfi, M. Lusi, D. Paolucci, M. Polito, K. Rubini and F. Grepioni, *Chem. – Eur. J.*, 2007, **13**, 5249–5255.
33 A. N. Chekhlov, *Russ. J. Coord. Chem.*, 2009, **35**, 492–495.
34 A. Verma, M. Guino-O, M. Gillett-Kunnath, W. Teng and K. Ruhlandt-Senge, *Z. Anorg. Allg. Chem.*, 2009, **635**, 903–913.
35 U. Englich, K. Ruhlandt-Senge and F. Uhlig, *J. Organomet. Chem.*, 2000, **613**, 139–147.
36 R. H. Crabtree, *The Organometallic Chemistry of the Transition Metals*, John Wiley & Sons, Ltd., Hoboken, NJ, 4th edn, 2005.
37 A. N. Swinburne and J. W. Steed, *Podands. Supramolecular Chemistry: From Molecules to Nanomaterials*, John Wiley & Sons, Ltd., see DOI: 10.1002/9780470661345.smc058.
38 P. C. Junk, L. M. Louis and M. K. Smith, *Z. Anorg. Allg. Chem.*, 2002, **628**, 1196–1209.
39 P. C. Junk and J. W. Steed, *J. Coord. Chem.*, 2007, **60**, 1017–1028.
40 W. Maudez and K. M. Fromm, *Z. Anorg. Allg. Chem.*, 2012, **638**, 1810–1819.
41 J. S. Alexander and K. Ruhlandt-Senge, *Chem. – Eur. J.*, 2004, **10**, 1274–1280.
42 M. R. Crimmin, A. G. M. Barrett, M. S. Hill, P. B. Hitchcock and P. A. Procopiou, *Inorg. Chem.*, 2007, **46**, 10410–10415.
43 K. Ruhlandt-Senge and U. Englich, *Chem. – Eur. J.*, 2000, **6**, 4063–4070.
44 B. Wei, Y. Tinant, M. Declercq, J. Van Meerssche and J. Dale, *Acta Crystallogr., Sect. C: Cryst. Struct. Commun.*, 1988, **44**, 77–80.
45 J. H. Burns, *Inorg. Chim. Acta*, 1985, **102**, 15–21.
46 W. A. Wojtczak, M. J. Hampden-Smith and E. N. Duesler, *Inorg. Chem.*, 1998, **37**, 1781–1790.
47 T. S. Pochekutova, V. K. Khamylov, Y. A. Kurskii, G. K. Fukin and B. I. Petrov, *Polyhedron*, 2010, **29**, 1381–1386.
48 M.-M. Zhao, *Acta Crystallogr., Sect. E: Struct. Rep. Online*, 2012, **68**, m286–m286.
49 L. Archer, M. J. Hampden-Smith and E. Duesler, *Polyhedron*, 1998, **17**, 713–723.
50 H.-F. Ji, R. Dabestani, G. M. Brown and R. L. Hettich, *J. Chem. Soc., Perkin Trans. 2*, 2001, 585–591.
51 S. Harder, B. Freitag, P. Stegner, J. Pahl and D. Naglav, *Z. Anorg. Allg. Chem.*, 2015, **641**, 2129–2134.
52 A. Steiner, G. T. Lawson, B. Walfort, D. Leusser and D. Stalke, *J. Chem. Soc., Dalton Trans.*, 2001, 219–221.
53 K. Reuter, G. Thiele, T. Hafner, F. Uhlig and C. von Hänisch, *Chem. Commun.*, 2016, **52**, 13265–13268.
54 (*a*) Turbomole Version 7.0.1, Turbomole GmbH 2016. Turbomole is a development of University of Karlsruhe and Forschungszentrum Karlsruhe 1989–2007, Turbomole GmbH since 2007; (*b*) F. Furche, R. Ahlrichs, C. Hättig, W. Klopper, M. Sierka and F. Weigend, *Wiley Interdiscip. Rev.: Comput. Mol. Sci.*, 2014, **4**, 91–100.
55 (*a*) F. Weigend and R. Ahlrichs, *Phys. Chem. Chem. Phys.*, 2005, **7**, 3297; (*b*) F. Weigend, *Phys. Chem. Chem. Phys.*, 2006, **8**, 1057; (*c*) M. Dolg, H. Stoll, A. Savin and H. Preuss, *Theor. Chim. Acta*, 1989, **75**, 173; (*d*) H. Stoll, B. Metz and M. Dolg, *J. Comput. Chem.*, 2002, **23**, 767; (*e*) S. Grimme, J. Antony, S. Ehrlich and H. Krieg, *J. Chem. Phys.*, 2010, **132**, 154104; (*f*) S. Grimme, S. Ehrlich and I. Goerigk, *J. Comput. Chem.*, 2011, **32**, 1456.
56 G. M. Sheldrick, *Acta Crystallogr., Sect. A: Fundam. Crystallogr.*, 2015, **71**, 3–8.
57 G. M. Sheldrick, *Acta Crystallogr., Sect. C: Cryst. Struct. Commun.*, 2015, **71**, 3–8.
58 O. V. Dolomanov, L. J. Bourhis, R. J. Gildea, J. A. K. Howard and H. Puschmann, *J. Appl. Crystallogr.*, 2009, **42**, 339–341.
59 D. Kratzert, J. J. Holstein and I. Krossing, *J. Appl. Crystallogr.*, 2015, **48**, 933–938.
60 Bruker, *SADABS*, Bruker AXS Inc., Madison, Wisconsin, USA, 2014.
61 Stoe & Cie, *X-AREA and X-RED32*, Stoe & Cie, Darmstadt, Germany, 2009.